

1179

(NASA-CR-176710) THEORETICAL AND MATERIAL
STUDIES ON THIN-FILM ELECTROLUMINESCENT
DEVICES Monthly Report, 1 Apr. - 30 Sep.
1985 (Georgia Inst. of Tech.) 47 p
HC A03/MF A01

N86-24905
Unclassified
CSCL 09A G3/33 43012

THEORETICAL AND MATERIAL STUDIES ON THIN-FILM
ELECTROLUMINESCENT DEVICES

First Six Month Report for the Period
1 April 1985 - 30 September 1985

Project No. A-4168

Prepared for:

Dr. J. B. Robertson/494
NASA
Langley Research Center
Hampton, VA 23665



Prepared by:

Dr. C. J. Summers* and Dr. K. F. Brennan⁺
Georgia Institute of Technology
Atlanta, GA 30332

February 1986

*Georgia Tech Research Institute and Microelectronics
Research Center

+School of Electrical Engineering and Microelectronics
Research Center

CONTENTS

	<u>Page No.</u>
1. INTRODUCTION	1
2. ELECTROLUMINESCENT DEVICES	3
2.1 Thin-Film Electroluminescent Devices.	3
2.2 Charge Carrier Transport and Multiplication .	8
2.3 Properties of the Luminescent Center.	11
2.4 Properties of Insulator and Electrodes. . . .	20
2.5 Material Properties for Electroluminescent Devices	22
3. DEVICE MODELING STUDY - ELECTRON ENERGY DISTRIBUTION FOR ZnSe	25
4. A NEW STRUCTURE FOR ELECTROLUMINESCENT DEVICES . .	33
5. SUMMARY	41
6. REFERENCES	42

LIST OF FIGURES

<u>Figure</u>	<u>Page No.</u>
1. Schematic of thin-film electroluminescent device.	4
2. Illustration of operation of thin-film electro-luminescent device, depicting hot electron and impact excitation processes.	6
3. Electron scattering rate vs. electron energy for GaAs at 300K.	7
4. Impact ionization process in a direct bandgap semiconductor.	9
5. Energy level scheme for ground and excited states of Mn-ion in ZnS lattice.	12
6. ZnS:Mn brightness and decay time as a function of Mn doping concentration.	14
7. Comparison of Tb and TbF ₃ doping behavior in ZnS as a function of Tb/Zn mole fraction.	18
8. ZnS:TbF ₃ brightness and decay time as a function of Tb doping.	19
9. Energy band structure for ZnSe. The conduction band shape was derived from a pseudopotential calculation, and the valence band estimated from the results obtained on other materials.	26
10. Dependence of density states on energy for ZnSe at 300K.	27
11. Dependence of electron scattering rate on energy for ZnSe at 300K.	28
12. Dependence of steady state on electric field for ZnSe at 300K.	30
13. Dependence of normalized distribution function of hot electrons on electron energy for ZnSe at 300K under an accelerating field of 500 kV/cm.	31
14. Illustration of variably spaced superlattice injection scheme. (a) Device geometry, (b) Zero bias, (c) Applied bias, eV=E ₁	34

LIST OF FIGURES

LIST OF TABLES

<u>Table</u>		<u>Page No.</u>
1.	Luminescent Center for ZnS.....	16
2.	Best Host Material/Luminescent Center Combinations for Electroluminescent Devices ..	21

1. INTRODUCTION

There is a strong need for better color displays in aircraft and space shuttle work stations as well as many applications for these devices in industry, commerce, and entertainment. At present, these needs are satisfied by the cathode ray tube (CRT) and, in some limited situations, by light emitting diodes (LED's) and liquid crystal devices (LCD's). Unfortunately, the latter two devices are severely limited in their color capabilities. For example, there is no viable blue LED available, and LCD's can only offer a change in contrast. However, these devices do have significant advantages; they can be operated at low voltages, and fabricated as thin panels. Thus they are compatible with integrated circuits and their fabrication technology. Also these devices are extremely rugged, long lived, and light. These advantages make them ideally suited for aerospace applications and in situations where a flat display screen is desirable. In contrast, the cathode ray tube is a high voltage relatively bulky device, and requires supporting electronics which add significantly to its size and weight. In addition, for high contrast applications and in adverse environments its operating lifetime is limited. However, its display capabilities, color and screen size, are unmatched by any other type of device which accounts for its dominance of this market for the last three decades.

Recently, there has been a renewed interest in thin-film electroluminescent display devices. These devices operate at intermediate voltages (200-300 volts), display all the primary colors (red, green and blue), can be fabricated as large area flat panels (8 x 8 inches), and have exhibited long lifetimes under adverse environments. Essentially, these devices consist of a thin semiconducting film which acts as the host for the luminescent center and provides the source of high energy electrons to excite the center. The most common material system is ZnS:Mn which emits in the yellow region of the spectrum. The problem with these devices is that their efficiencies are very

low resulting in poor picture contrast, and it is difficult to accommodate different color centers in the same or compatible host lattices. Conventionally, these devices are grown by evaporation to form amorphous undoped and doped layers which are then annealed to promote more efficient luminescent devices. The use of crystalline semiconductor films has also been shown to result in higher efficiencies. If further improvements could be obtained, then these structures would stand a realistic chance of competing with CRT displays.

The long range objective of this program is therefore to perform a comprehensive theoretical and experimental study of EL devices with the specific objectives to:

- (1) Identify the fundamental physical mechanisms responsible for controlling device operation.
- (2) Identify the material parameters necessary to optimize device performance.
- (3) Grow and characterize relevant materials and device structures.
- (4) Investigate new device concepts for EL-devices.

As a necessary requirement to perform these studies a comprehensive review of the present understanding and state-of-the-art of these devices was performed in the first phase of this work (Section 2) and was followed by some exploratory device modeling studies (Section 3). As discussed in the test, these activities resulted in the invention of a new device concept, the variable spaced superlattice energy filter (VSSEF) device which provides a mechanism for efficient high energy carrier injection in EL and other types of device. This concept is presented in Section 4.

2. ELECTROLUMINESCENT DEVICES

Electroluminescence occurs by two basic mechanisms, low field EL based on minority carrier injection as in light emitting diodes, and high field EL based on acceleration of majority carriers, typically electrons, to optical energies at which luminescent centers can be impact excited.^{1,2} High field EL was first reported in ZnS³ and since has been investigated in a host of new materials as an application of new thin film technology.⁴⁻¹⁰ Two basic device schemes using a.c. and d.c. power have been realized to date and are discussed in detail below.

2.1 Thin-Film Electroluminescent Devices

Typical a.c. electroluminescent devices are made by encapsulating a large band gap semiconductor, such as ZnS:Mn or ZnSe:Mn, by two insulating layers, typically Y₂O₃, on either side of the semiconductor layer.

Thus, as shown in Figure 1, a typical thin-film electroluminescent device is a symmetrical insulator-semiconductor-insulator sandwich which produces light when biased by a high electric field.¹ The key ingredient of the structure is the high resistivity semiconductor layer which contains the active luminescent centers and is also the medium for the transport of hot electrons. At high electric fields electrons trapped at the first insulator-semiconductor interface or in deep acceptor states in the insulating layers are excited from these states and tunnel into the conduction band or the semiconductor.¹⁰ Here they are accelerated (heated) by the electric field and gain energy. For hot electrons with sufficient energy impact-excitation of active luminescent center can occur.^{4,11} In this process the hot electron transfers its energy to an electron in the ground state of the atom thus elevating it to an excited state. This causes a population inversion in the center which is reversed when the electron falls back to the ground state with the emission of a photon.^{12,13} Thus the electrical energy in the device is converted to light.

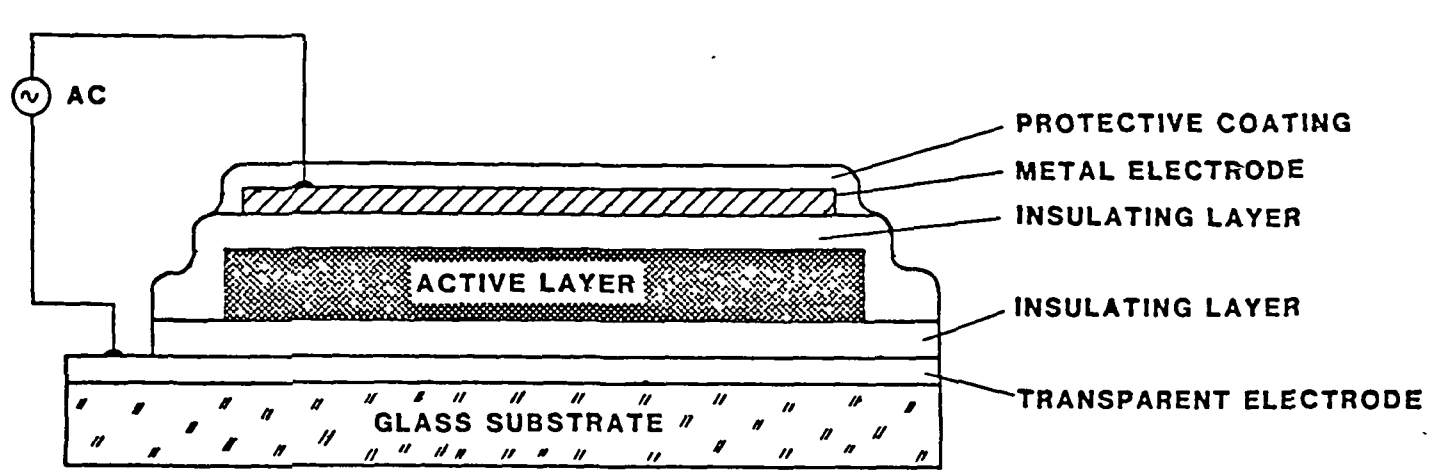


Figure 1. Schematic of thin-film electroluminescent device.

Those electrons which are not captured by the luminescent center continue to traverse the structure and collect near the anode. This causes a positive space charge in the second insulator which hinders the transport of further electrons across the device. Consequently, the electron density across the semiconductor region decreases and the light output falls. However, if the polarity of the external voltage is reversed, the action of the reversed electric field in the device is two-fold. New electrons are injected into the device from the second semiconductor-insulator interface, and these electrons and the electrons trapped near the second electrode are accelerated back into the semiconductor layer by the combined field due to the external applied voltage and the space charge. The increased electron population will thus produce a higher emission.¹ By alternately switching the voltage, increased light output can be obtained until the generation of electrons equals their loss by recombination processes in the structure. Thus the probability of an electron impact exciting a center depends upon the collision cross section and the density of centers in the semiconductor layer as well as the probability of an electron achieving the impact excitation threshold energy.

The efficiency of the device is thus dependent on the properties of the luminescent center, host lattice, and cladding insulator; and the way in which the device is operated. To optimize these devices therefore, a greater understanding is required of the physical mechanisms controlling carrier generation, charge transport and multiplication, the impact excitation process, the recombination properties of the luminescent center, and the functions of the insulating and contacting layers of the device.

A brief discussion of some of these factors and material properties required to optimize current device structures are discussed in the following sections of this report. Calculations of hot electron effects in EL materials and new device concepts are discussed at the end of the report.

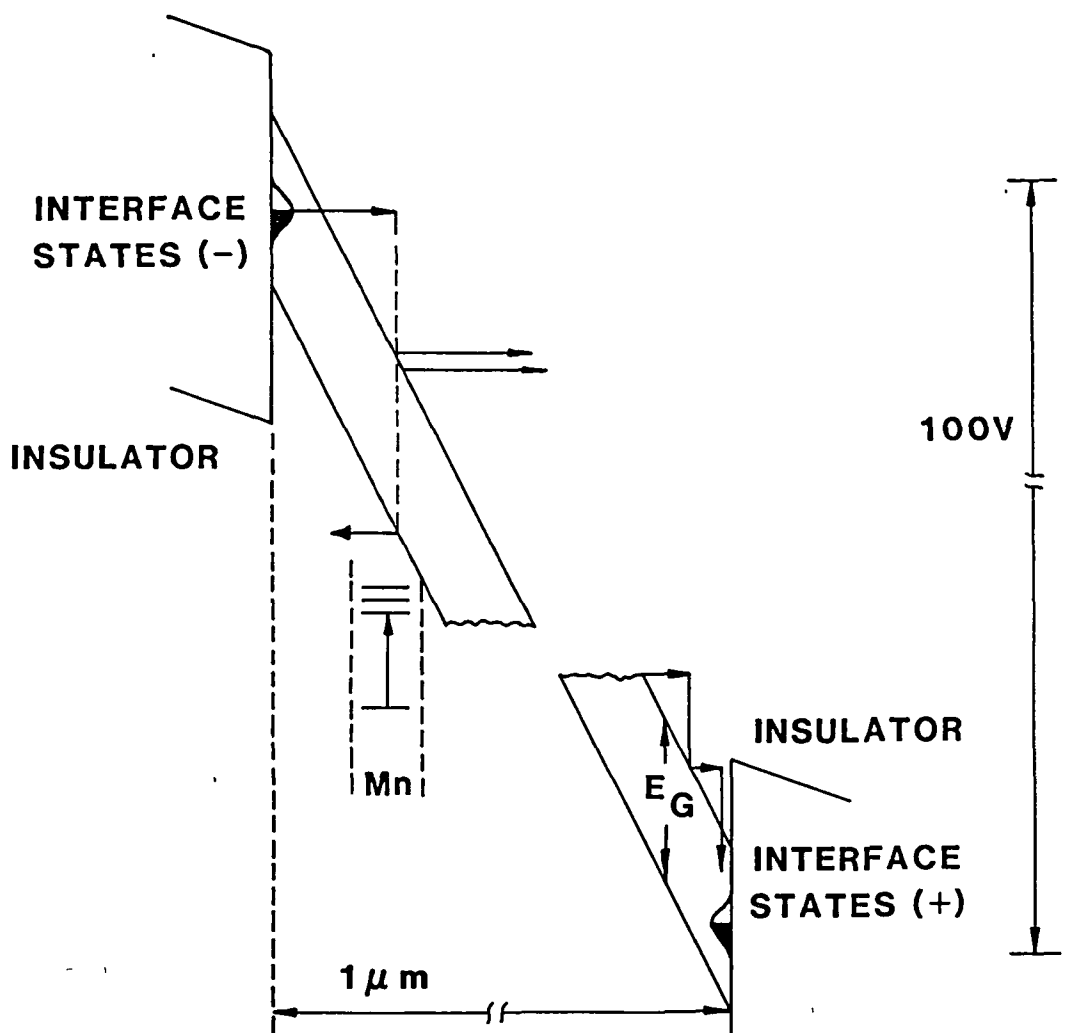


Figure 2. Illustration of operation of thin-film electroluminescent device, depicting hot electron and impact excitation processes.

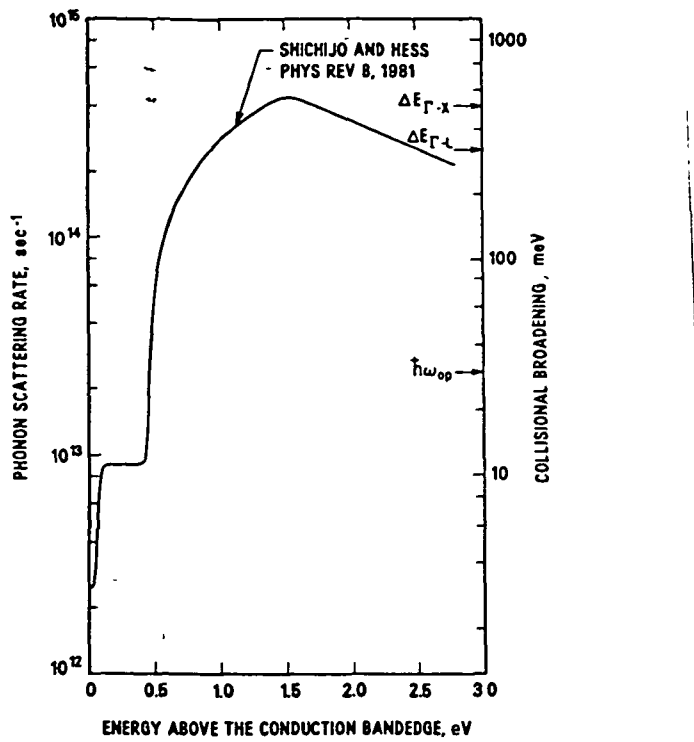


Figure 3. Electron scattering rate vs. electron energy for GaAs at 300K.

2.2 Charge Carrier Transport and Multiplication

The mechanisms of carrier transport in a semiconductor are very dependent on the carrier energy as has been realized from steady-state studies of hot-electron phenomena in semiconductors.¹⁴ The factors which contribute to this dependence have recently been succinctly summarized and discussed by Hess and are shown in Figure 3 for GaAs at 300K.¹⁵

For small applied voltages in which the average energy of the electron distribution is less than the energy of an optical phonon the electrons are scattered by acoustic and optical phonons and impurities. In this regime, the carrier transport is ohmic. As the electric field increases, the average electron energy becomes greater than the optical phonon energy. For this situation, an order of magnitude decrease occurs in the energy relaxation time because electrons can now lose energy by the emission of optical phonons. This loss process is very efficient and dominates the energy relaxation time until the average electron energy approaches the separation between the conduction band minimum at $k=0$ and the minimum in the $\langle 111 \rangle$ valley at high k -values. Above this energy, electrons are efficiently scattered into the $\langle 111 \rangle$ valley by the electron deformation potential and the scattering rate increases to 10^{14} events/s. Finally, for a further increase in the average electron energy a significant number of electrons gain enough energy to induce impact ionization and thus charge carrier multiplication. For this process, the energy of the hot electron must exceed a threshold value which is slightly greater than the bandgap energy (Figure 4). Thus in an impact with a valence electron the hot electron transfers its energy to the valence electron, exciting it to the bottom of the conduction band while it simultaneously also falls to the bottom of the conduction band. Thus an extra conduction electron and a hole is produced, resulting in charge multiplication.

The entire process is then repeated resulting in a further increase in the concentration of hot electrons. This mechanism is very efficient and can produce gains up to 1000 in a Si

IMPACT IONIZATION PROCESS

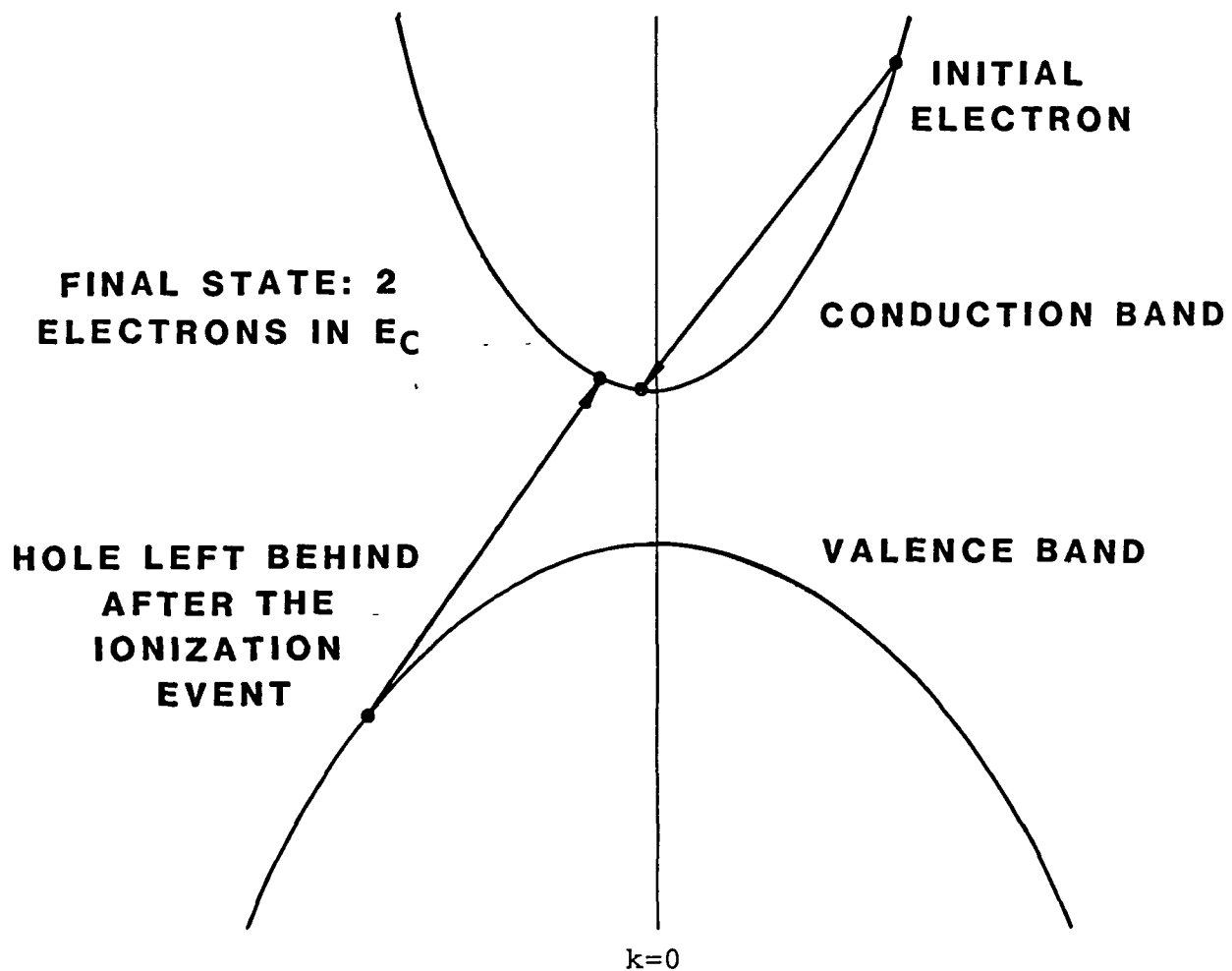


Figure 4. Impact ionization process in a direct bandgap semiconductor.

detector. However, gains of only 10 have been observed in thin-film EL devices. This relatively low multiplication factor is attributed to the wider bandgap and polycrystalline nature of the EL material.

It should also be noted that although charge multiplication is produced, the energy distribution of carrier is heavily weighted to low energies. Thus only a very small fraction of charge carriers have sufficient energy to impact ionize or impact-excite a luminescent center.

The interactive nature of the carrier scattering, heating and gain processes are very complicated and strongly dependent on the semiconductor band structure. To obtain an accurate description of the transport processes in a high field therefore requires use of the Monte Carlo techniques as described in Section 3.

Electroluminescence is produced by a similar process which occurs when a hot electron with energy, E_{ex} , collides with a luminescent center. In this impact-excitation mechanism the hot electron transfers its energy to the center by exciting an electron in the ground state of the center to a higher excited state; while it simultaneously falls to the bottom of the conduction band. Latter recombination of the excited electron with the hole in the ground state occurs by either radiative or non-radiative recombination. In the first process light is produced, while in the second, the energy of the electron hole pair is lost as heat to the lattice. These processes are shown schematically in Figure 5. Obviously, for efficient luminescence, the second process must be made negligible. Additionally, to obtain efficient excitation of the luminescent center, the impact excitation energy of the center, E_{ex} , must be less than E_G in order not to compete with the intrinsic mechanisms in the layer and to take advantage of the charge carrier multiplication processes. Also because the energy of the optical emission is usually only slightly less than the impact excitation energy of the center, the condition $E_{ex} < E_G$ is required to prevent the emitted radiation from being absorbed by the host crystal.

However, the most significant factor which limits the efficiency of current devices is the large mismatch between the energy distribution of the hot electrons and excitation spectrum of the luminescent centers. Because the excitation spectrum of the luminescent center is approximately monochromatic, the number of electrons that can interact with the center is limited as a consequence of their broad distribution which is heavily weighted to low energies. This puts a fundamental limit on the excitation efficiency. To increase the number of excited centers, either the total number of hot electrons must be increased, or the efficiency of the impact excitation process must be improved. In the first approach, the basic mechanisms are optimized by the correct choice of material properties and possibly by using the intrinsic avalanche process to multiply the number of electrons. This could be achieved by using separate avalanching and doped layers so as to optimize each process. In the second approach, the electron distribution must be altered and made to match the excitation spectrum of the center. A means for accomplishing this may be possible by using superlattice structures which are designed to restrict the electron distribution into narrow energy segments, as discussed in Section 4.

2.3 Properties of the Luminescent Center

The properties of the luminescent center in the semiconductor must also satisfy stringent conditions to produce an efficient device. The emission wavelength is determined by both the properties of the center and its interaction with the host lattice. For example, as shown by Figure 5 for Mn in ZnS, the crystalline field of the zinc-blende structure splits both the excited and ground states of the Mn-atom and breaks down the optical selection rules such that efficient recombination rates are now possible between these states.^{12,13} The detailed properties of this situation are difficult to predict accurately and still require considerable experimental verification, both for the Mn center, and particularly for new center-host crystal

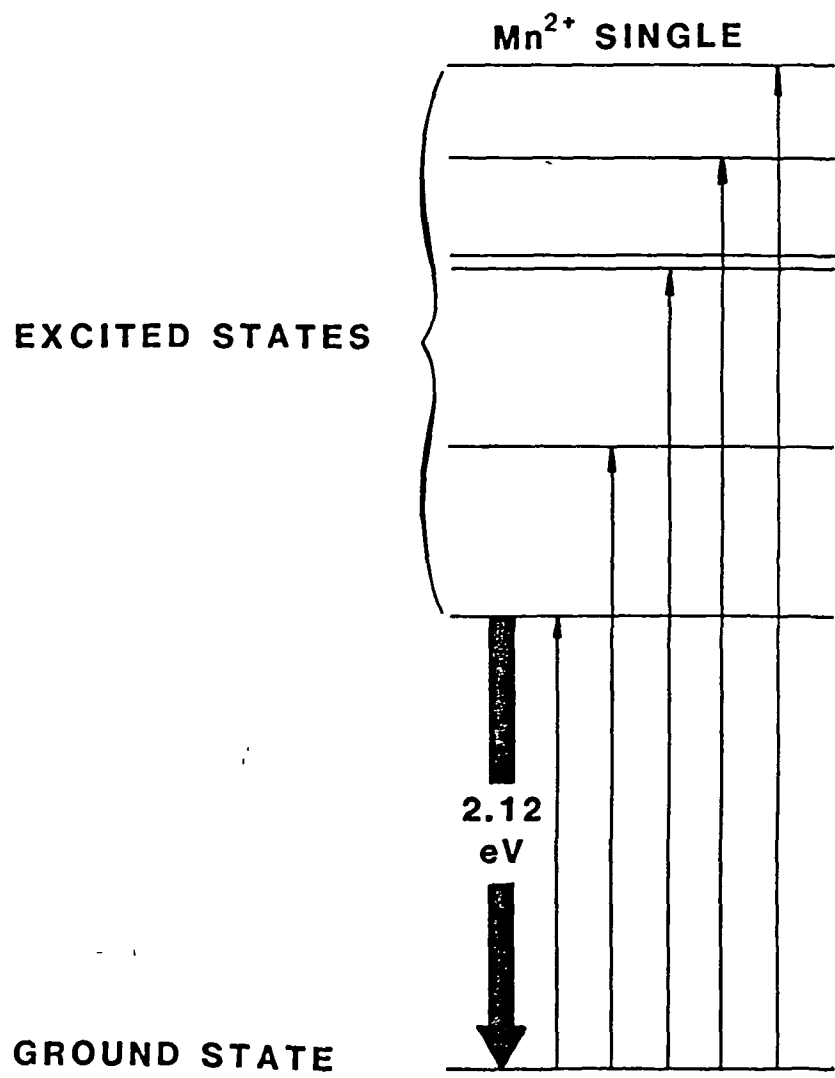


Figure 5. Energy level scheme for ground and excited states of Mn-ion in ZnS lattice.

combinations.

In addition to the above mentioned physical requirements, the center must be highly soluble in the host lattice to increase the number of electron-center interactions and luminescence output, and to preserve the operating wavelength and integrity of the structure the inner shell electronic structure must be well shielded from the electric field. Finally, the device stability is greatly improved if the center is isovalent, or neutral, in the host lattice so as to avoid ion drift under the action of the high electric fields.

Despite the fact that it is one of the most efficient luminescent centers, the behavior of Mn is still not understood. As shown in Figure 6, the intensity of the luminescence emitted by the Mn center is strongly dependent on the Mn concentration. Initially, the luminescent intensity increases linearly with Mn concentration reaching a maximum at a concentration of approximately 1%. For higher concentrations, the luminescence intensity decreases rapidly and is almost completely quenched for Mn concentrations exceeding 2%. Figure 6 also shows that the decay time of the luminescence decreases continuously with increasing Mn concentration. The saturation and ultimate quenching of the luminescence with increasing Mn concentration has been attributed by Kreitman and Bennett¹⁶ to the formation Mn-Mn pairs and triplets on next-to nearest Zn sites. For Mn concentrations greater than 1%, these complexes are calculated to include 20 and 10%, respectively, of the total Mn concentration. Thus their formation is expected to have a strong influence on the luminescent properties of the center. It is postulated that at higher Mn concentrations an excited center can transfer its energy to another Mn atom thus raising it to an excited level. This phenomenon means that the excitation can travel through the crystal, thus increasing its probability of encountering a non-radiative center or decay path and being annihilated. An alternative proposal for the decrease in luminescent intensity with increasing Mn concentration is that the interaction between centers allows Auger-transitions to occur thus producing a rapid

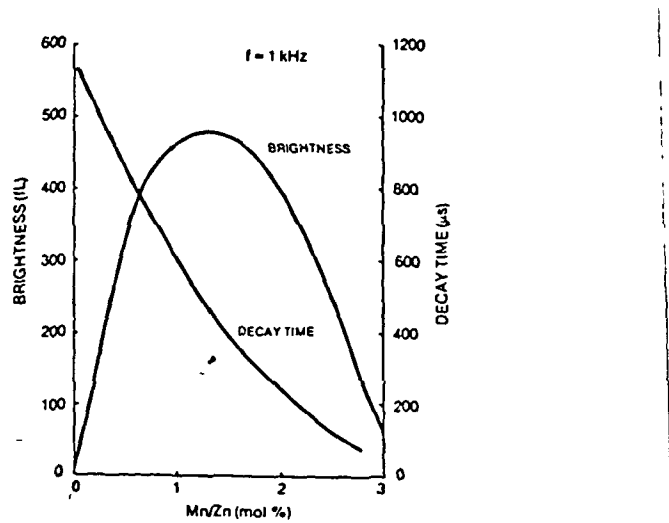


Figure 6. $Z_{ns}:\text{Mn}$ brightness and decay time as a function of Mn doping concentration.

quenching of the luminescence and radiative decay time. Both of these processes are thought at present to have equal merit and thus more experimental work is required in this area on well characterized materials in order to quantify the mechanisms responsible for the observed behavior.

Of the other dopants investigated in ZnS for luminescent applications, the Rare-earths have been the most successful as listed in Table 1. As observed, erbium, holium and terbium produce emission in the green, Tm in the blue, Sm and Nd in the red, and Dy in the yellow.

All of this data was obtained for a typical MISIM structure (Figure 1) in which the Y_2O_3 and ZnS layers were deposited by evaporation or sputtering at low temperature on a glass substrate coated with ITO (InSnO). The dopants being introduced at the appropriate time by opening the shutter of a thermal evaporation dopant source. Thus the structures are either amorphous or only partially crystalline. The luminescence measurements were also made for standard comparison conditions for the THEL Display industry by using a a.c. voltage bias at 5 kHz. Because for practical applications a 60 Hz bias is required, the values at this frequency are also given. As demonstrated by the table, these values are more than a factor of 30 below the higher frequency values and demonstrate the necessity for significantly higher brightness and efficiencies for all phosphors.

The first study of these centers by Okamoto showed that although a variety of wavelengths (colors) could be obtained their efficiencies were very low.^{17,18}

Initially, it was assumed that this was a consequence of a smaller cross-section for the electron impact-excitation of rare-earth atoms. This assumption was based on the fact that the energy levels associated with the emission from rare-earth luminescent centers are internal f-levels whereas for Mn the more outer d-levels are involved. However, calculations by Bernard et.al.¹⁹ indicated that the electron capture cross-sections for the rare-earths and Mn should be very similar, indicating that the lower efficiencies are produced by non-radiative channels

Table 1. Luminescent Centers for ZnS

Dopant	Color	Brightness 5 kHz	(ft.lum.) 60 Hz
Mn	Yellow	1500	30
ErF ₃	Green	60	0.74
DyF ₃	Yellow	140	1.68
HoF ₃	Green	70	0.84
TbF ₃	Green	500 (2000)	6.00(44)
SmF ₃	Red	200	2.40
TmF ₃	Blue	2	0.02
NdF ₃	Red	6	0.07

caused by the non-ideal incorporation of trivalent rare-earth atoms into the ZnS lattice. Recent research has therefore focused on varying the processing details and the use of co-activators with the correct valency in order to achieve higher luminescent efficiencies.

The use of coactivators to balance the valence caused when a luminescent center is added to a material is commonly used to increase the luminescence of CRT phosphors and also has been demonstrated in ZnS. For example, the emission from Cu doped ZnS can be enhanced by the addition of a halide. Because Cu is monovalent and substitutes on the Zn lattice, the simultaneous substitutions of a halide atom on the S lattice provides an extra electron to compensate for electron deficiency caused by Cu doping. An alternative co-activator scheme is the use of trivalent aluminum which substitutes on an adjacent Zn atom. Now the one electron from Cu and the three from Al equal the four electrons provided by the two Zn atoms they replace thus ensuring electrical neutrality in the lattice.

The effectiveness of fluorine to behave as a coactivator for Tb is demonstrated in Figure 7. As shown, for just Tb doping of ZnS the luminescent output reaches a maximum for a doping level of 3% mole fraction of Tb substituting for Zn and then slowly decreases for increasing Tb concentration up to a mole fraction of 7%.

In contrast, Figure 8 also shows the significantly higher brightness and its strong dependence on Tb concentration up to doping levels of 9% mole fractions of Tb. In addition, as demonstrated by Figure 8, the emission decay time continues to increase at higher Tb dopant concentrations. This behavior is distinctly different from that observed in Mn doped ZnS and is attributed to the fact that the presence of high concentrations of F coactivators which increase the probability of the excitation energy being transferred from one Tb-F center to another instead of encountering a non-radiative recombination channel. Thus higher luminescent efficiencies and longer decay lifetimes are observed and increase with TbF_3 concentration.

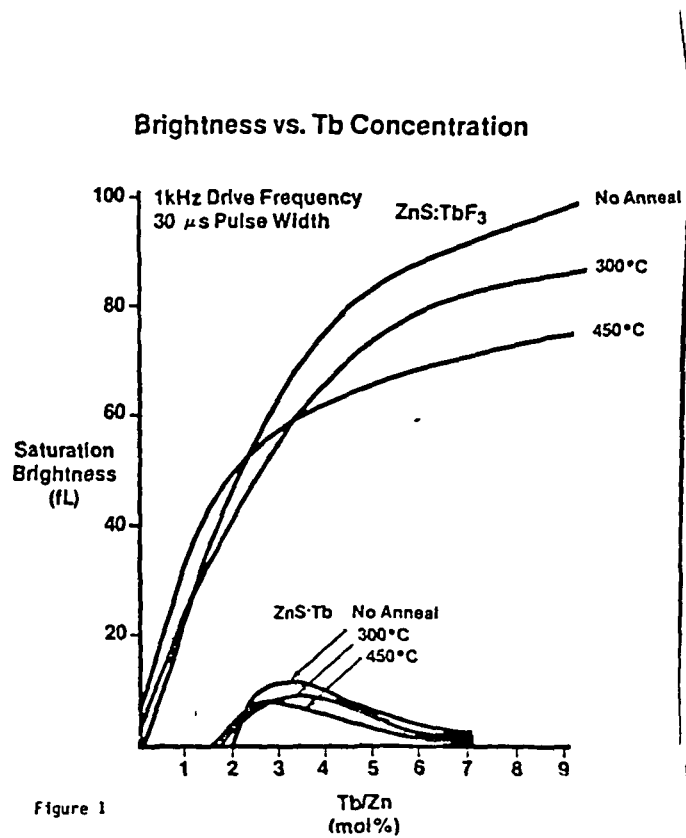


Figure 7. Comparison of Tb and TbF_3 doping behavior in ZnS as a function of $\text{Tb}/2n$ mole fraction.

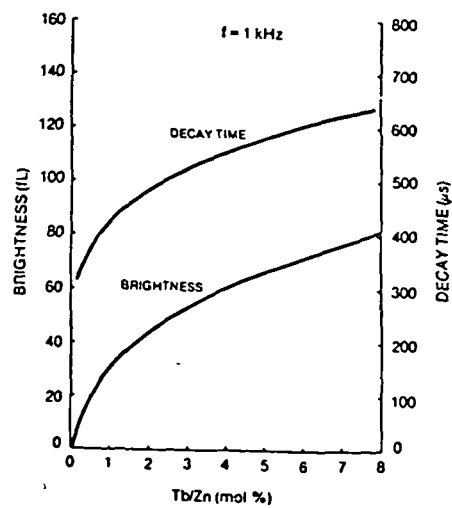


Figure 8. $\text{ZnS}:\text{TbF}_3$ brightness and decay time as a function of Tb doping.

It should also be noted that the structural incorporation of the luminescent center or complex into the host lattice has a strong effect on the luminescent efficiency. For example, a non-uniform distribution of the dopant and poor crystallinity and density of the host/center film severely limits the performance. Thus frequently a variety of annealing procedures are used to improve the film quality and therefore luminescent output after evaporation or sputter deposition. Because there is a large number of reported recipes with an equally wide range of results, these procedures will not be mentioned in detail, although as shown by Figure 7, it can be seen that these procedures are not always beneficial.

As mentioned previously, Mn has been found to be the most efficient center and luminescences in the yellow region of the spectrum. Attempts to obtain different colors by using rare-earth dopants in the ZnS lattice have produced green and red emission characteristics, but unfortunately with significantly lower brightness and efficiencies than other systems. Whether these efficiencies can be improved requires further study, but this work does demonstrate that a range of colors are possible by using different centers in the same lattice.

Because of its efficiency and compatibility with II-VI semiconductors Mn has also been used as an active center in ZnSe and CdF₂ and found to produce orange and green luminescence, respectively. However, again lower efficiencies have been observed than with some other systems. Thus attempts to produce a range of colors by using different centers in the same lattice, or the same center in different host lattices have had some success, but have not produced the highest brightness for each color. At present, the most efficient systems are ZnS:Mn, ZnS:TbF₃²¹, SrS:Eu and SrS:CeF₃²² for the yellow, green, red and blue, respectively. (Table 2).

2.4 Properties of the Insulator and Electrode Films

The purpose of the insulating films is to stabilize the device during the period in which avalanching (dielectric

Table 2. Best Host Material/Luminescent Center Combinations for Electroluminescent Devices

Material	Color	Brightness 5 kHz	(ft.lum.) 60 Hz
ZnS:Mn	Yellow	1500	30
ZnS:TbF ₃	Green	2000	44
SrS:Eu	Red	300	3
SrS:CeF ₃	Blue	250	3

breakdown) occurs in the semiconducting layer. Thus the layer must have high dielectric strength (a high breakdown voltage) and to minimize the voltage drop across the layer during operation a high value for the static dielectric constant. This will cause most of the applied voltage to be dropped across the semiconducting layer resulting in lower operating voltages and higher efficiencies.

Ohmic contacts must also be formed to the device to minimize unnecessary voltage drops. This can be accomplished either by using a fine metal grid or preferably an optically transparent highly conductive film such as indium-tin oxide. This has the advantage of equally distributing the high voltage bias across the device thus reducing localized breakdown effects and producing a more uniform and efficient light output.

The techniques for producing good oxide and electrode films are well documented and thus will not be actively investigated in this proposal.

2.5 Material Properties for Electroluminescent Devices

The previous reviews show that although sufficient information is known about each mechanism to give a qualitative description of each process, quantitative descriptions of the most important mechanisms are not available, either because of their complexity or because they have not been studied in detail. The quality of the materials studied has also severely limited precise measurements of many of the physical mechanisms controlling the performance characteristics of these devices.

A review of a recent conference on Display Technology also strongly suggests that the Display industry is intent on improving the performance of display devices by refining current technologies.

This approach has shown some promising results by the development of some new phosphors and host lattice combinations with higher brightness and suggests that the commercialization of these devices may soon be possible. However, these devices will still require a high voltage A.C. bias (~200v, 5 kHz) to obtain

the required performance, which will limit their use to special applications. It was also apparent at this conference, and from a review of the literature that there is very little work directed at understanding in detail the physical mechanisms which control device operation. This, we believe, is a serious omission as it means that the basic information required to make long term improvements in device performance and which is also required to enable a breakthrough in this field will not be available.

As discussed previously, the performance of thin-film electroluminescent devices is very dependent on a number of complex and interacting physical mechanisms; specifically the generation of hot electrons and the use of charge multiplication techniques to increase their density, the impact-excitation process, the recombination processes of the luminescent center, and the properties of the insulating and electrode films and interfaces between layers.

Currently, the quantum and power efficiencies are very low, typically less than 1% and 0.1%, respectively. These very low values result from the following problems.

1. The density of electrons traversing the active layer is very low, typically between 10^{10} - 10^{11} cm $^{-3}$. This is because interface and deep levels provide a very limited and uncontrollable source of electrons and because at present it is difficult to obtain high multiplication factors in these structures.
2. The hot electron distribution is extended over a wide range of energies such that only a relatively small number of electrons have sufficient energy to impact-excite a luminescent center.
3. The electron impact-excitation cross-section of the centers is relatively small.

4. The radiative and non-radiative recombination mechanisms of the centers have not been fully documented and are unknown for high concentrations of luminescent centers.

Of these factors, the generation of a high density of hot electrons represents a major limitation to the performance efficiency of thin-film electroluminescent devices. To overcome this problem, we have therefore proposed a novel variably spaced superlattice energy filter (VSSEF) device which provides high energy injection of near monoenergetic electrons into a bulk semiconductor layer at any energy tuned to the impact-excitation of the luminescent center. This concept should result in a dramatic increase in the efficiency and brightness of TFEL devices with the additional advantage of low voltage D.C. operation. In fact, it is possible that if the theoretical expectations are realized, the operating conditions required for this device concept could make it compatible with silicon integrated circuits. The full details of this scheme are described in Section 4 following a description of a calculation of the hot electron distribution in ZnSe.

3. DEVICE MODELING STUDY-ELECTRON ENERGY DISTRIBUTION FOR ZnSe

Operation of electroluminescent devices depends critically upon the excitation of high energy transitions within the luminescent centers. Overall device efficiency, optical power out (brightness) per input electrical power, is related to both how efficiently the electrons are heated to the luminescent center excitation energy and how efficient the excitation process is. Theoretical studies of the behavior of electroluminescent devices therefore center on the accurate determination of the electron energy distribution function and the impact excitation cross section.

The electron distribution function can be calculated within the host semiconductor through solution of the Boltzman Transport Equation, BTE. We have numerically solved the BTE using the Monte Carlo method which is based on a stochastic simulation of the electron transport history. The technique we employ is unique in that the full details of the conduction band structure (first two conduction bands) is included. A parabolic model of the energy band structure, $E = \frac{h^2 k^2}{2m}$, is insufficiently accurate to describe the transport dynamics at very high carrier energies. In addition, the full details of the electron-phonon scattering mechanisms (polar optical, acoustic, intervalley deformation potential, and impact ionization) are treated using a rigorous quantum mechanical calculation (collisional broadening).

The first conduction band as well as a representative sketch of the valence bands in ZnSe is presented in Figure 9. The conduction band is derived from a pseudopotential calculation. The density of states of both the first and second conduction bands is shown in Figure 10. The "camel-back" feature of the density of states curve is due to the fact that the first and second conduction bands have their maximum density of states at quite different energies. This is of great significance to the electron-phonon scattering rate since deformation potential scattering is directly proportional to the final density of

ZnSe BAND STRUCTURE

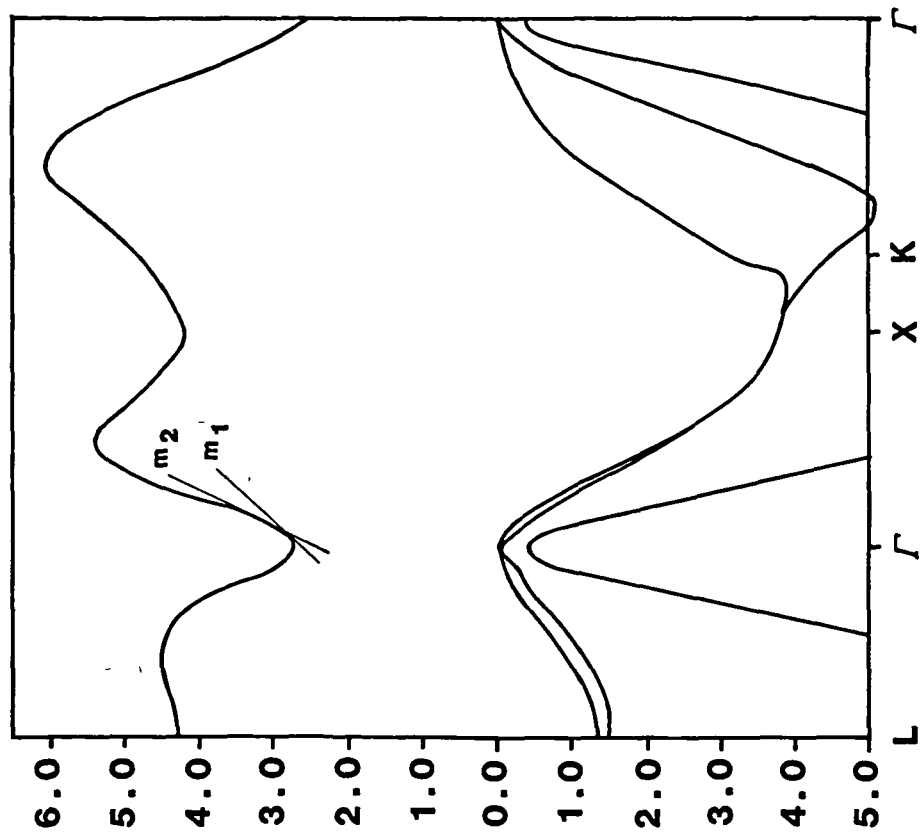


Figure 9. Energy band structure for ZnSe. The conduction band shape was derived from a pseudopotential calculation, and the valence band estimated from the results obtained on other materials.

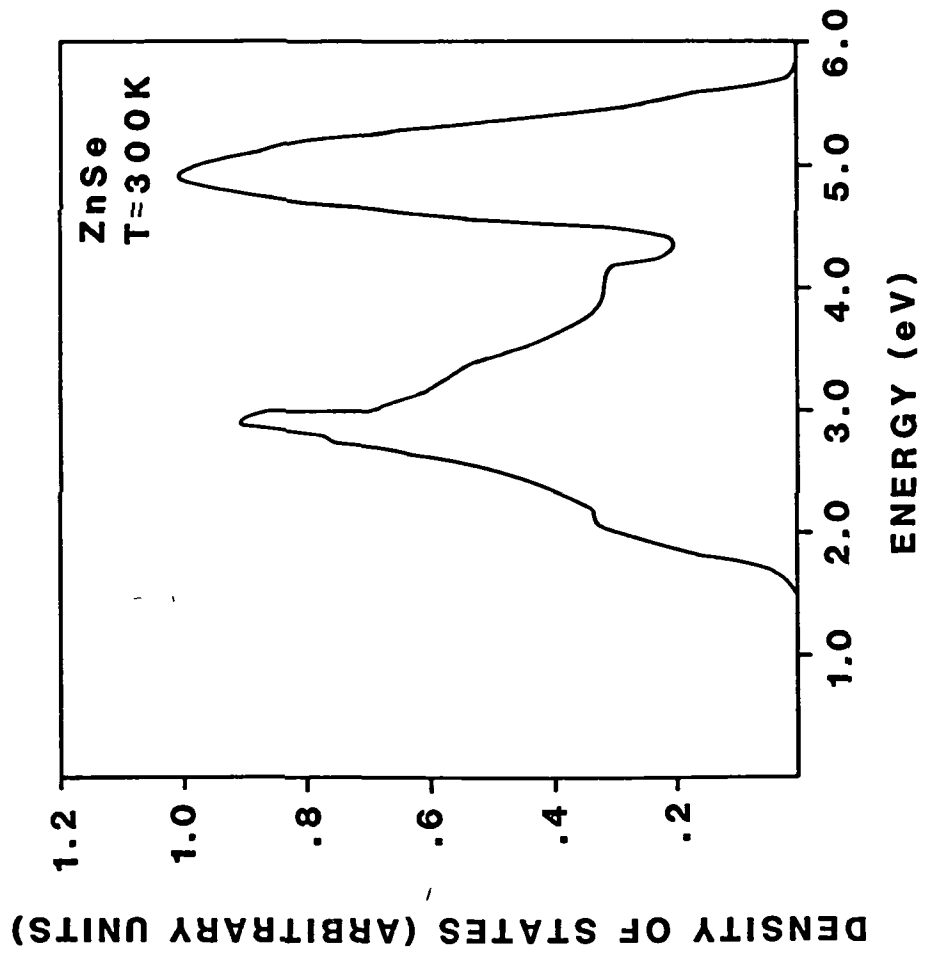


Figure 10. Dependence of density states on energy for ZnSe at 300K.

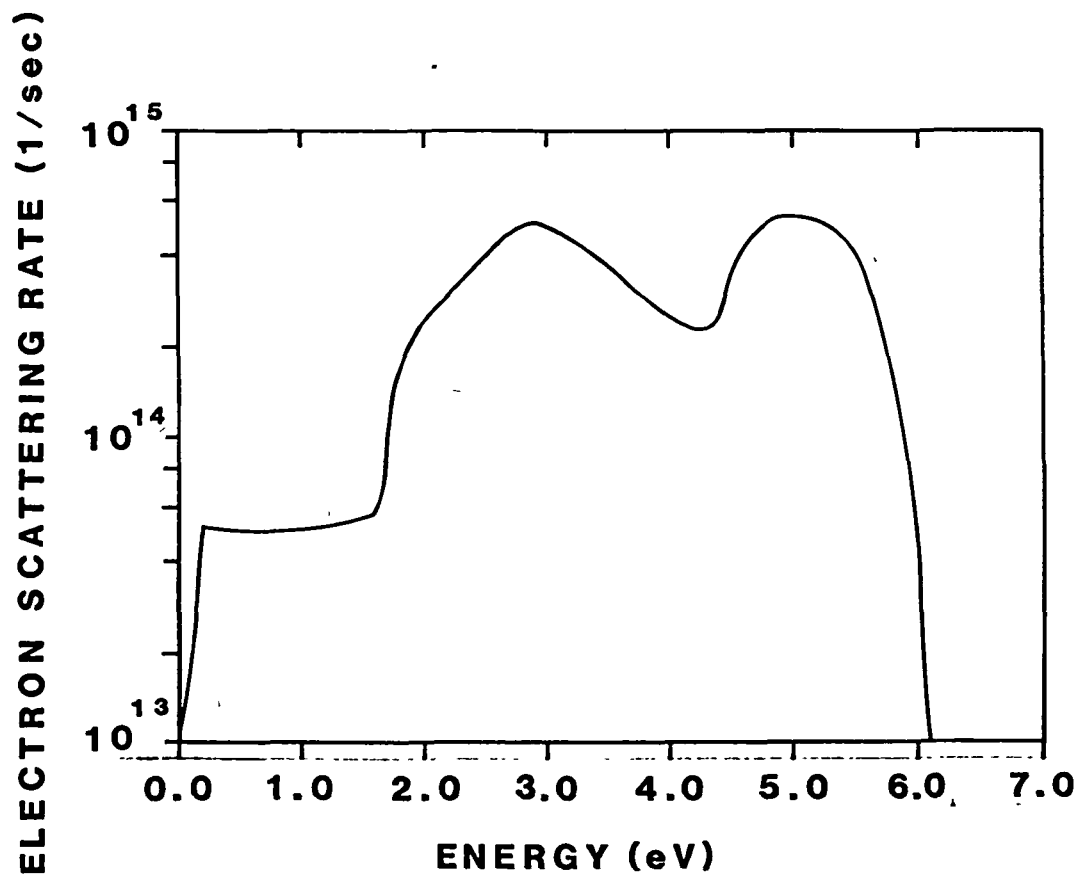


Figure 11. Dependence of electron scattering rate on energy for ZnSe at 300K.

states. Consequently, as shown in Figure 11, the electron-phonon scattering rate goes through a minimum where the density of states decreases. In ZnSe this occurs at ~4.0eV. If the impact ionization process has a "soft threshold" (meaning that the electrons need drift to substantially higher energies than threshold before they ionize on average) then the tail of the energy distribution function extends well into this region. As shown in Figure 12, then the carrier drift velocity begins to increase again with field rather than saturate. Conversely, if the impact ionization threshold energy is "hard" (electrons ionize readily upon attaining threshold) the electron drift velocity tends to saturate (points marked with squares in Figure 12). Recent theoretical work in other material systems, silicon, GaAs, and InP suggests that the ionization threshold is "soft" thus predicting that both the carrier drift velocity will not saturate at high fields and more importantly to EL devices that the tail of the distribution function will extend to very high energies.

Figure 13 is a plot of the normalized electron energy distribution function calculated within ZnSe at an applied field of 500 kV/cm at 300°K. The distribution is weighted by the density of states function. In order to determine then the number distribution the product of the energy distribution and the density of states must be formed. It is interesting to note that even at an applied field of 500 kV/cm only a small fraction (~.5%) of the electrons have an energy equal to that of the excitation energy. Consequently, the heating of electrons to energies necessary for electroluminescent excitation is very inefficient if accomplished solely by use of an applied field. The explanation of this is simple. Under the application of a steady-state electric field the electron energy is balanced by energy loss through phonon interactions. Hence few electrons overcome, on average, the substantial cooling effects of phonon emission resulting in a vanishingly small population of higher energy carriers.

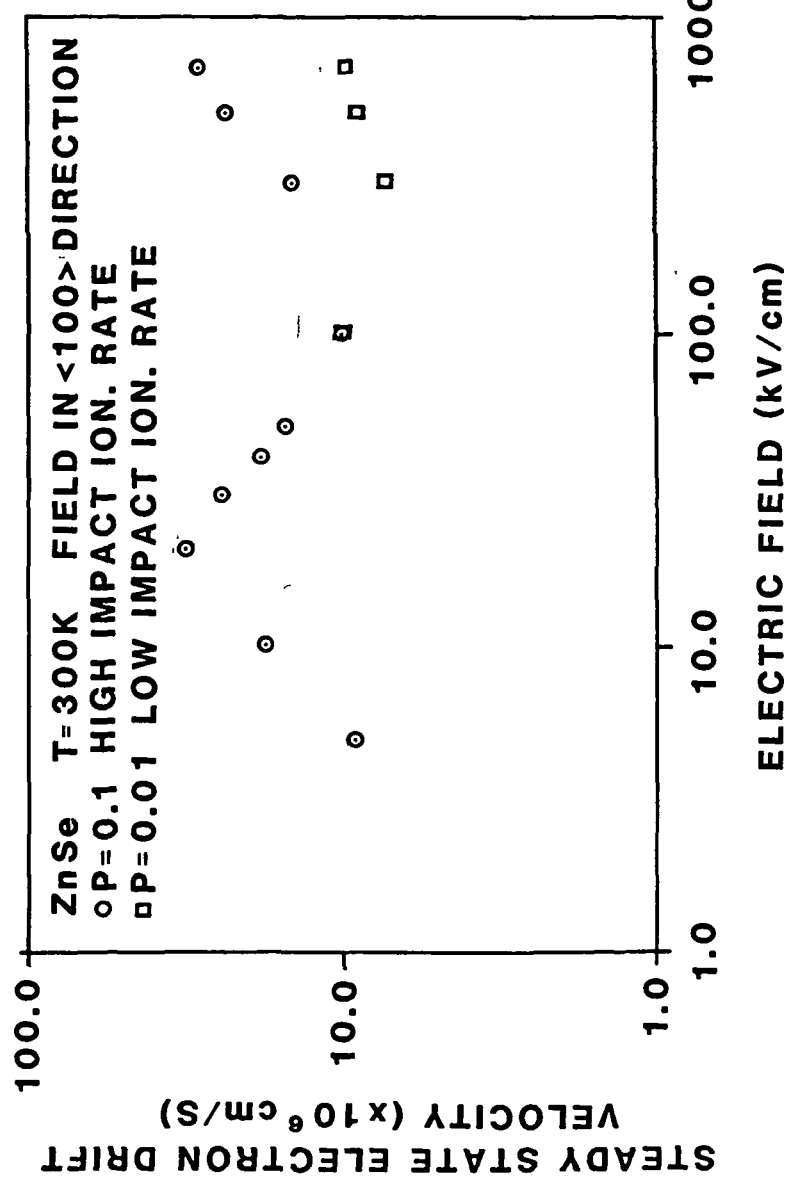


Figure 12. Dependence of steady state on electric field for ZnSe at 300K.

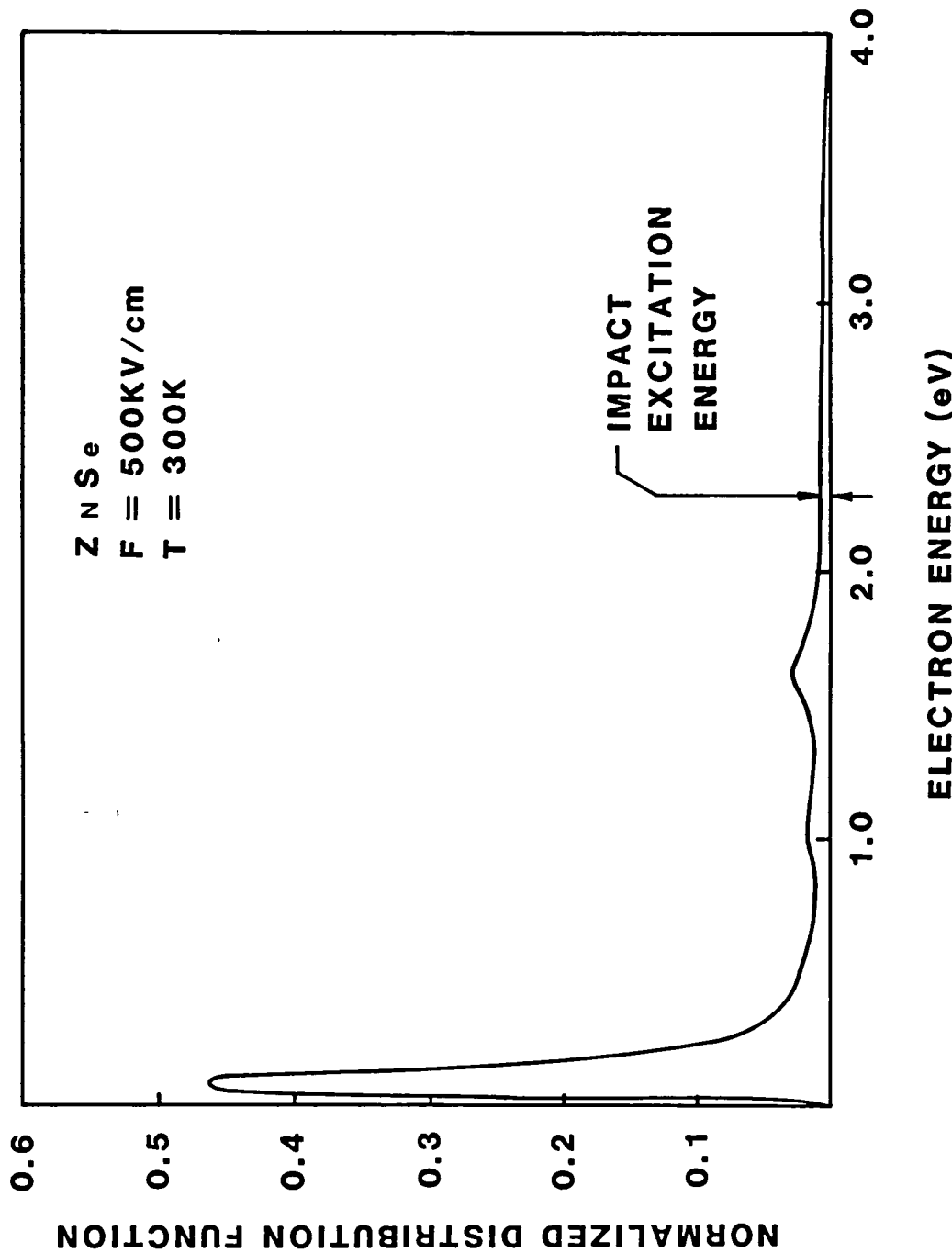


Figure 13. Dependence of normalized distribution function of hot electrons on electron energy for ZnSe at 300K under an accelerating field of 500 KV/cm.

4. A NEW STRUCTURE FOR ELECTROLUMINESCENT DEVICES

In this section, a new variably spaced superlattice energy filter (VSSEF) is described which provides for high energy injection of electrons into a bulk semiconductor layer based on resonant tunneling between adjacent quantum well levels which are brought into alignment by an applied bias. Applications of this concept, to thin film electroluminescent devices and other devices such as APDs and IMPATTs are also discussed. As described in many texts, the performance of all of these devices depends critically upon the efficient production of high energy, hot electrons.²³⁻²⁷ Carrier heating is achieved by application of high electric fields and is balanced on average by inelastic scattering processes. Consequently, high voltages are required to produce a significant high energy electron concentration. A more efficient means of carrier heating is by high energy injection from a heterostructure,^{28,29} but is extremely difficult to achieve in wide bandgap material systems without producing carrier pile-up effects.³⁰ We propose a new device concept, the variably spaced superlattice energy filter (VSSEF), which provides a novel means of injecting high energy electrons.

The proposed device, as shown in Figure 14 under zero and reverse bias, consists of a variably spaced superlattice (SL) formed from alternating layers of a semiconductor of bandgap E_{g1} and a larger bandgap semiconductor or insulator of bandgap E_{g2} . These materials form the quantum wells (QWs) and barrier layers of the structure respectively, and must satisfy the condition that the conduction band edge discontinuity be large. High majority carrier concentrations are provided through use of an n^+ semiconductor or metal contact to the first barrier layer. The active layer of the device into which the hot electrons are injected immediately follows the last QW and barrier and is contacted by an n^+ or p^+ -type semiconductor, or metal layer.

The SL structure is designed such that under reverse bias the levels in each QW are closely aligned with each other, and with the Fermi level in the n-type electrode. This energy level

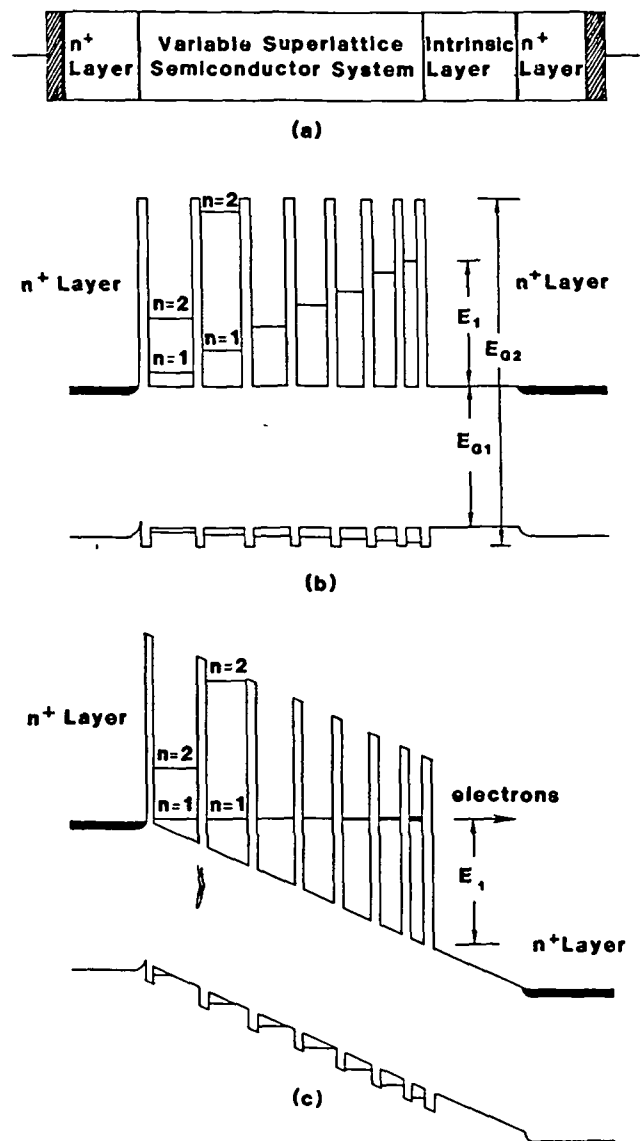


Figure 14. Illustration of variably spaced superlattice injection scheme. (a) Device geometry, (b) Zero bias, (c) Applied bias, $eV \sim E_1$.

scheme is obtained by a judicious choice of well thickness and barrier widths, such that electrons can tunnel through the first thin insulator layer into the first QW of the SL and then continue to resonantly tunnel from one QW to the next. Thus in the simplest implementation of the proposed scheme, electrons are injected into the conduction band of the active semiconductor layer at an energy E_1 above the conduction band edge, where E_1 is the energy of the first subband in the last quantum well. Throughout the structure, the QW widths are designed such that the bound states lie at an energy equal to the voltage drop between any two adjacent wells, and the barrier widths are optimized to enhance the resonant tunneling between adjacent wells. Thus the VSSEF device affords high energy injection by providing a tunneling channel in a biased superlattice.

The variable SL can be modeled using the infinite square well approximation, in which the energy levels are given by,

$$E_n = \frac{\pi^2 \hbar^2}{2m^*} \frac{n^2}{L^2} , \quad n = 1, 2, \dots \quad (1)$$

where L is the well width, n the level index, and m^* the effective mass of the low bandgap material.

Equation (1) quite accurately predicts the position of the low energy states, but as shown by Dingle,³¹ a finite square well calculation is necessary for the high energy states near the end of the SL.

Typical hot electron devices in moderate to wide bandgap materials require carrier energies of 1.5-3.0 eV and thus E_1 must be in this range. Consequently, the conduction bandgap difference between the two materials must be much larger than E_1 . The most demanding test of this concept is its application to thin film EL displays which require that $E_1 = 2.7$ eV to impact excite blue luminescent centers.^{32,33} For an injection energy of 2.7 eV and an effective mass of a typical wide bandgap (ZnS or ZnSe) semiconductor, the width of the last QW is 7 Å. Well widths

this small are not in general considered to be technically feasible. Also the discrete interatomic spacing prevents fine tuning of the allowed subband energies. These limitations can be circumvented, however, by using energy levels with $n > 1$. For $E = 2.7$ eV, well widths of 28, 63, 112, and 175 Å corresponding to $n = 2, 3, 4, 5$ are predicted using the infinite square well approximation. Thus for $n > 2$ the crucial device parameters fall within the predicted MBE technology goals. This conclusion has been confirmed by an exact finite square well calculation which shows that for the worst case the last well will be 50% narrower than the values given above. Similar calculations for a GaAs well show that 1.5 eV electrons can be obtained for the first energy level in a 20 Å well provided a suitable insulator can be found.

The predominant carrier transport mechanism within the SL structure arises from resonant tunneling between the aligned quantum levels in adjacent quantum wells. The tunneling is strongly dependent on the barrier widths and can be rigorously calculated using the method of Vassell et al.³⁴ As shown by Stratton,³⁵ in a metal-insulator-metal system, significant tunneling currents are achievable even for 50 Å wide barriers. However, in the device proposed here the potential barrier height is larger than that considered by Stratton which may necessitate the use of narrower barriers.

The subband energy spacings are proportional to the square of the level index (Eq.1). Thus for $n > 1$, the energy level separation becomes $\gg kT$. These conditions ensure that very few electrons thermalize to lower energy states before tunneling to the adjacent well. Since the electric field, arising from the voltage drop necessary to align the quantum levels, is along the direction of quantization, carrier heating by the field cannot occur because there is no continuum of states available. Heating can only occur if sufficient energy is available for the electrons to be excited from one quantum level to the next, or if electrons can be scattered orthogonal to the field where the electronic structure has its conventional parabolic dependence on

k. The probability of both of these events is small.

Thermionic emission of carriers from the quantum well states over the barriers provides the only other possible mechanism of conduction and can be prevented by using high bandgap insulators. A more critical limitation on device performance could arise if the electric field severely limits the tunneling probability between wells.^{36,37} However, as shown by Bastard,³⁷ the electron wavefunctions are not severely distorted even at extremely high fields, ~100 kV/cm, and thus this does not appear to be a problem.

The narrow QWs at the end of the structure cause the levels to be significantly broadened. This has the beneficial effect of easing the alignment conditions for the subbands and possibly enabling the electrons to gain some kinetic energy at the end of the structure from the applied electric field. Even if it proves impossible to construct a series of wells which align to the same energy under bias, nonresonant phonon assisted tunneling or hopping^{38,39} can still occur and be stimulated by the field. Since the speed of response of the device is not critical this should not present any serious limitations.

The utility of the VSSEF device is that it produces high energy injection of monoenergetic electrons into a semiconductor. As such, it differs from Capasso et al's.⁴⁰ suggestion to use SLs for artificially inducing bandgap grading and as effective mass filters.^{40,41} This concept is also significantly different from the recent work of Capasso et al.⁴¹ and Nakagawa et al.^{43,44} who propose using SLs to produce a negative differential resistance. The CHIRP device proposed by Nakagawa et al.^{43,44} uses a Kronig-Penney potential to introduce a forbidden mini-gap at energies above the conduction bands of both constituents of the SL to produce a voltage sensitive transmission coefficient. Under the correct bias, the forbidden mini-gap aligns such that the emitted electrons must now tunnel through the full length of the SL. Since the tunneling current decreases with barrier width, the current decreases with bias resulting in a negative differential resistance. This effect has recently been experimentally

observed by Nakagawa et al.⁴⁵

The VSSEF device uses resonant tunneling both to channel the electrons through the device and to inject them at a very high energy into an adjacent semiconductor layer. Efficient high energy injection is obtained by reducing the energy lost to phonon processes by channeling the electrons between adjacent quantum levels. Therefore, they cannot lose energy to phonons since no states are available for the electrons to scatter into. The SL provides an alignment of successive quantum levels such that the electrons continuously gain potential energy (the applied electric potential inverts the superlattice) until they are finally injected into the active semiconductor region at extremely high kinetic energy.

Upon injection into the semiconductor, the distribution is initially monoenergetic, broadened only by the quantum mechanical energy broadening of the levels. The distribution will relax quickly by inelastic phonon scattering processes if the electric field is not large (Figure 15). Further heating can be achieved however, either by using a field across an intrinsic layer or a fully depleted built in p-i-n layer.

The hot electrons injected into the active semiconductor layer can be used in a variety of applications. For example, E_1 can be tuned to match the impact excitation energy of luminescent centers in thin film EL devices. Alternatively, the basic device scheme can be used in an avalanche photodetector by injecting electrons at high enough energy to impact ionize. Successive superlattice/semiconductor stages can then provide periodic and spatially deterministic electron ionization at low hole ionization. Consequently, high gain at low noise performance can be achieved. Additionally, these structures have the important advantage of low voltage operation, <5.0 volts.

Finally, we note that material systems and MBE growth techniques exist for implementing these concepts. For EL applications a variety of perfectly lattice-matched ZnSSe:CaSrF₂ SL structures are possible with energy gaps of $Eg_1 = 2.7 - 3.6$ eV, $Eg_2 = 11.44 - 12.2$ eV. This range should enable large

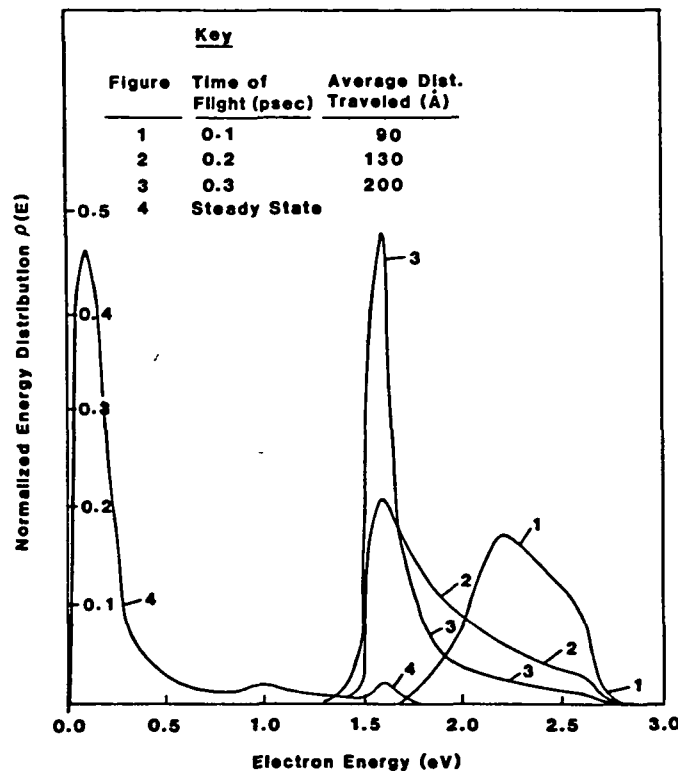


Figure 15. Monte Carlo calculation of electron energy distribution in ZnSe at $T=300K$ following high energy injection at 2.58 eV. The distribution is weighted by the density of states. The "bunching up" of the distribution at 1.50 eV is due to the low scattering rate from L and X to Γ . The applied field of 30 kV/cm is below the intervalley threshold field ~ 40 kV/cm, which results from the large intervalley separation energies, ~ 1.50 eV.

conduction band edge discontinuities to be achieved even if the energy gap difference is equally shared between the conduction and valence bands. Similarly, a range of GaAs-flouride SLs are possible for both detector and IMPATT applications. Optimum VSSEF APD structures should also be possible using the CdTe:HgCdTe SL system in which the lattice match and valence band alignment is very close. More extensive studies of the applications of this concept to thin film EL devices, APDs and IMPATT structures, as well as the negative differential resistance properties of the structure will be published in future work.

5. SUMMARY

During this report period we have performed a detailed assessment of current EL materials and device technology as outlined in Section 2. This evaluation strongly suggests the need for a comprehensive theoretical and experimental study of both materials and device structures, particularly in the following areas:

- o carrier generation and multiplication
- o radiative and non-radiative processes of luminescent centers
- o device modeling
- o new device concepts
- o single crystal materials growth and characterization

A significant start has been made in modeling the transport properties of hot electrons in ZnSe and the generation of new and novel device concepts. A paper describing the physical principles of the VSSEF device has recently been accepted by Applied Physics Letters and we are considering applying for a patent for this idea. We strongly believe that the possibilities of the VSSEF structure should be more fully explored and that subsequently this structure should be grown. Thus more detailed analyses of this structure are in progress, and our MBE growth program is being extended to do this. More details of these endeavors will be given in the Final Report.

6. REFERENCES

1. R. Mach and G. O. Muller, Physical Concepts of High-Field, Thin-Film Electroluminescence Devices, Phys. Stat. Sol. (a) 62, 11-66 (1982).
2. F. Williams, J. of Luminescence, 23 (1981), 1.
3. G. Destriau, J. de Chemie Physique, 33 (1936), 620.
4. M. Mach, W. Gerricke, H. Treptow, and W. Ludwig, Phys. Stat. Sol. (a), 49, (1978), 667.
5. D. C. Morton and F. E. Williams, Appl. Phys. Lett., 35, (1979), 671.
6. K. Okamoto and Y. Hamakawa, Appl. Phys. Lett. 35, (1979), 508.
7. J. Benoit, P. Benalloul, R. Parrot and J. Matther, J. of Luminescence, 18/19 (1979), 739.
8. H. Ohnishi, H. Yoshino, K. Ieyasu, N. Sakuma, and Y. Hamakawa, Proceedings of the SID, 25/3 (1984), 193.
9. F. J. Bryant, A. Krier, and G. Z. Zhong, Solid-State Electronics, 28 (1985), 847.
10. S. Smith International Workshop on Electroluminescence, Liege, 1980. J. Lum.
11. D. A. Cuseno, Luminescence of Organic and Anorganic Materials, Ed. Kallman and Spruch, Wiley, New York (1962).
12. H. E. Gumlich, Sammlung, Vieweg. Branschweig 1970.
13. H. E. Gumlich, R. L. Pfrogner, J. C. Shafer and F. E. Williams, J. Chem. Phys. 44 3929 (1966).
14. S. Sze. Semiconductor Device Physics, J. Wiley, 1965.
15. H. Shichijo and K. Hess, Phys. Rev. B 23, 4197 (1981).
16. M. M. Kreitman and D. L. Bennett, J. Chem. Phys., 43, 364 (1965).
17. K. Okamoto, Thesis, Osaka University (1981).
18. K. Okamoto and Y. Hamokawa, Appl. Phys. Lett., 35, 508 (1979).
19. J. E. Bernard, M. F. Martens, D. C. Morton and F. Williams.

20. R. T. Tuenge, R. E. Coovert and W. A. Barrow, Extended Abstracts, 159, Electrochemical Soc. Meeting, 422 (1981).
21. H. Ohnishi, H. Yoshino, K. Ieyasu, N. Sakuma, and Y. Hamakawa, Green-emitting thin-film dc EL devices with low threshold voltage, Proc. SID 25, 193-199 (1984).
22. J. B. Robertson, private communication.
23. G. E. Stillman, V. M. Robbins, and N. Tabatabaie, IEEE Trans. Electron Dev., ED-31, 1643 (1984).
24. F. Capasso, in Lightwave Communications Technology, and Semimetals, (R. K. Willardson and A. C. Beers, eds.) (Academic Press, New York, 1985), p. 1.
25. P. S. Barnes and W-H Su, unpublished.
26. R. Mach and G. O. Muller, Phys. Stat. Sol. (a), 69, 11 (1982).
27. F. Williams, J. of Luminescence, 23, 1 (1981).
28. J. Y. Tang and K. Hess, IEEE Trans. Electron Dev., ED-29, 1906 (1982).
29. R. Chin, N. Holonyak, G. E. Stillman, J. Y. Tang and K. Hess, Electron. Lett. 16, 467 (1980).
30. S. R. Forrest, O. K. Kim, and R. G. Smith, Solid State Electron., 26, 951 (1983).
31. R. Dingle, in Festkorperprobleme, edited by H. J. Queisser, Advances in Solid State Physics, Vol. 15 (Pergamon/Vieweg., Braunschweig, 1975), p. 21.
32. F. J. Bryant, A. Krier, G. Z. Zhong, Solid-State Electronics, 28, 847 (1985).
33. R. Okamoto and Y. Hamakawa, Appl. Phys. Lett., 35, 508 (1979).
34. M. O. Vassell, Johnson Lee, and H. F. Lockwood, J. of Appl. Phys., 54, 5206 (1983).
35. R. Stratton, J. Phys. Chem. Solids, 23, 1177 (1962).
36. G. H. Dohler, R. Tsu, and L. Esaki, Solid State Commun., 17, 317 (1975).
37. G. Bastard, Superlattices and Microstructures, 1, 265 (1985).
38. R. Tsu and G. Dohler, Phys. Rev. B., 12, 680 (1975).

39. D. Caleki, J. F. Palmier, and A. Chomette, *J. Phys. C.: Solid State Phys.*, **17**, 5017 (1984).
40. F. Capasso, H. M. Cox, A. L. Hutchinson, N. A. Olsson, and S. G. Hummel, *Appl. Phys. Lett.*, **45**, 1193 (1984).
41. F. Capasso, K. Mohammed, A. Y. Cho, R. Hull and A. L. Hutchinson, *Appl. Phys. Lett.*, **47**, 420 (1985).
42. F. Capasso and R. A. Kiehl, *J. Appl. Phys.*, **58**, 1366 (1985).
43. T. Nakagawa, N. J. Kawai, K. Ohta, M. Kawashima, *Electronics Letters*, **19**, 822 (1983).
44. T. Nakagawa, N. J. Kawai, K. Ohta, *Superlattices and Micro-structures*, **1**, 187 (1985).
45. T. Nakagawa, H. Imamoto, T. Sakamoto, T. Kojima, K. Ohta, and N. J. Kawai, *Electronics Letters*, **21**, 822 (1985).